Electrochemistry Communications 12 (2010) 583–586

Contents lists available at ScienceDirect

Electrochemistry Communications

journal homepage: www.elsevier.com/locate/elecom

Electrodeposition of rhodium onto a pre-treated glassy carbon surface

E.N. Schulz, D.R. Salinas, S.G. García *

Instituto de Ing. Electroquímica y Corrosión (INIEC), Departamento de Ingeniería Química, Universidad Nacional del Sur, Avda. Alem 1253, 8000 Bahía Blanca, Argentina

ARTICLE INFO

Article history:
Received 22 November 2009
Received in revised form 28 January 2010
Accepted 8 February 2010
Available online 11 February 2010

Keywords:
Glassy carbon substrate
Rhodium
Nucleation and growth
2D–3D transition

ABSTRACT

The electrodeposition of rhodium from a 0.5 M NaCl + 5 mM Na_3RhCl_6 solution onto an electrochemically activated glassy carbon (GC) electrode was investigated by cyclic voltammetry and chronoamperometry. The cyclic voltammogram showed the presence of two cathodic peaks associated with the deposition of Rh. The analysis of the chronoamperometric curves, according to the existing theories, indicated that the Rh electrodeposition can be explained by a combination of several nucleation processes: two-dimensional (2D) progressive nucleation, which transforms to 2D instantaneous nucleation at more cathodic potentials, followed by three-dimensional (3D) nucleation with diffusion controlled growth. The nucleation kinetic parameters were determined according to these theories.

1. Introduction

Rhodium is a well-known metal belonging to the platinum group, which has many important industrial applications and shows outstanding catalytic properties for various reactions such as the reduction of nitrate and nitrite ions [1]. Therefore, different authors have reported results concerning the electrochemical deposition of rhodium clusters and films onto different substrates, such as Au(1 0 0) and polycrystalline Au [2], polycrystalline Pt [3], Pt(1 0 0) and Pt(1 1 1) [4], highly oriented pyrolytic graphite (HOPG) [5] and non-treated glassy carbon electrode [6,7]. Rhodium is a very expensive metal; therefore, its electrodeposition onto a more economical substrate constitutes a way to prepare a competitive catalytic electrode. In this way, glassy carbon is a relatively low cost substrate and could be used as an electrocatalyst support. In addition, the possibility of enhancing the Rh deposits through a pre-activation treatment of the surface makes the glassy carbon a potential candidate for Rh applications on industrial scale. The electrochemical pre-treatment of GC through the oxidation and reduction of the electrode surface is one of the most commonly methods to improve the electrode response. This procedure leads to the increase in oxygen-containing functional groups which enhances the electron transfer and specific adsorption behaviours [8].

In the present work we present, for the first time, classical electrochemical experiments concerning the early stages of the Rh electrodeposition process onto an electrochemically activated glassy carbon (GC) surface, in order to gain further insight into the corresponding nucleation and growth mechanism.

2. Experimental

A GC rod sealed into a Teflon holder (area $A = 0.07\ cm^2$) was used as the working electrode. Prior to each experiment, the substrate surface was first mechanically polished with progressively finer emery paper and finally, with 0.3 μm particle size Al_2O_3 powder, until a mirror-like finished surface was obtained. Then, it was washed with fourfold quartz-distilled water. Cyclic polarization was employed for the activation of the glassy carbon electrode. The potential was cycled between +2 and −1 V vs. saturated calomel electrode (SCE) for eight cycles at $10\ mV\ s^{-1}$ in 0.5 M H_2SO_4 solution.

The Rh particles were electrodeposited onto the GC electrode from a 0.5 M NaCl + 5 mM Na_3RhCl_6 solution (pH 3.3) which was prepared from suprapure chemicals (Merck, Darmstadt) and fourfold quartz-distilled water. The electrolyte was deaerated by nitrogen bubbling prior to each experiment.

The electrochemical measurements were carried out at a temperature $T = 298$ K in a conventional three-electrode electrochemical cell. The counter electrode was a platinum sheet ($1\ cm^2$) and the reference electrode was a SCE mounted inside a Luggin capillary. All potentials in this study are referred to the SCE. The measurements were carried out with a potentiostat–galvanostat EG&G Princeton Applied Research Model 273A.

The kinetic parameters were obtained by a non-homoscedastic fitting of experimental data with the theoretical equations using a

* Corresponding author. Tel./fax: +54 291 4595182.
E-mail address: sgarcia@criba.edu.ar (S.G. García).

1388-2481/$ - see front matter © 2010 Elsevier B.V. All rights reserved.
doi:10.1016/j.elecom.2010.02.005

Microsoft Excel's Solver routine in conjunction with Maple 12 symbolic mathematics software.

3. Results and discussion

Fig. 1a shows the cyclic voltammograms for the activated and non-activated GC electrode obtained in a 0.5 M NaCl + 5 mM Na_3RhCl_6 solution, in the potential range $-900 \leqslant E/\text{mV} \leqslant 0.0$. The voltammogram for the case of a non-activated surface is similar to that recorded by Pletcher and Urbina [6]. During the negative-going sweep, two cathodic features are observed before the hydrogen evolution reaction, which is recorded at $E \leqslant -800$ mV. The well-defined steep peak I, clearly evident at $E_{p,I} = -330$ mV, was ascribed to the nucleation of Rh onto the glassy carbon surface followed by a rapid growth of the crystals. The slight shoulder (denoted as II), observed at more negative potentials ($E_{p,II} = -440$ mV) and the anodic peak III recorded on the reverse scan ($E_{p,III} = -330$ mV) were attributed [6] to the hydrogen adsorption/desorption onto the freshly deposited Rh particles, respectively. No anodic peaks related to the stripping of Rh are present because this metal does not dissolve anodically due to the formation of a passivating oxide layer. The cyclic voltammogram exhibits a crossover between the cathodic and anodic branches which is characteristic for the formation of Rh nuclei on the surface. The crossover potential, $E_{co} \approx -122$ mV, is not well defined due to the formation of the passivating oxide layer. Under charge transfer control and according to Fletcher et al. [9], the E_{co} value should correspond to the equilibrium potential of the metal redox couple. Nevertheless, in the present case, considering the passivation process and also that the solution contains a mixture of $[RhCl_n(H_2O)_{6-n}]^{(3-n)+}$ complexes with $[RhCl_5(H_2O)]^{2-}$ and $[RhCl_4(H_2O)_2]^{-}$ as the predominant species [6] it is very difficult to assign this potential to an equilibrium potential.

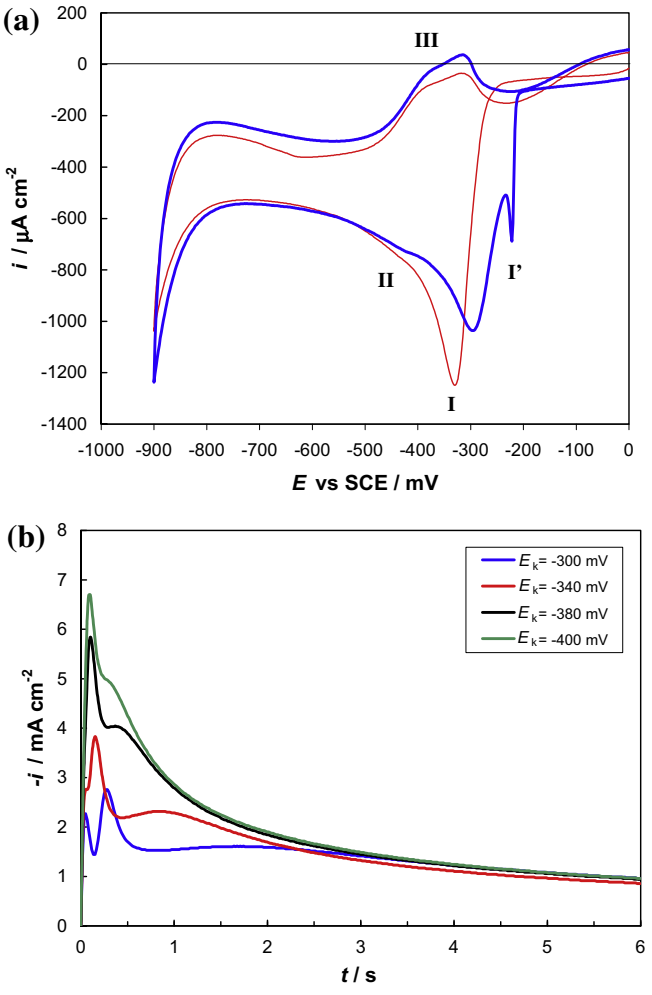

Fig. 1. (a) Cyclic voltammograms for the system GC/0.5 M NaCl + 5 mM Na_3RhCl_6 (pH 3.3) using non-activated GC (——) and activated GC (——). $|dE/dt| = 10$ mV s^{-1}. (b) Potentiostatic current density transients for the nucleation of Rh on activated GC at different potentials, E_k from $E_i = 0.0$ mV.

The voltammogram for the activated substrate shows that Rh electrodeposition initiates at relatively more positive potentials, with the appearance of a sharp cathodic peak I′ at $E_{p,I'} = -220$ mV. Additionally, peak I is also recorded at slightly more positive potential values. Pletcher and Urbina [6] have indicated that the Rh deposition on a non-activated GC surface follows a progressive nucleation mechanism with a three-dimensional (3D) growth of the nuclei under diffusion control. Therefore, the presence of peak I′ indicates a change of the deposition mechanism induced by the GC surface treatment.

Considering these voltammetric results, the nucleation process of Rh onto the activated GC electrode was analysed using the potential step technique. Fig. 1b shows a family of potentiostatic current transients obtained when the potential was stepped from $E_i = 0$ mV to more negative potential values, E_k, in the range $-400 \leqslant E_k/\text{mV} \leqslant -300$. After the initial current density increase due to the charging of the double layer, the transients exhibit a rising current density at short times, corresponding to the formation and growth of Rh nuclei, and a first peak is recorded. After this peak, at longer times, the transients exhibit the typical shape for a nucleation process with 3D growth of nuclei limited by diffusion of the electroactive species [10], i.e., the current increases due to the formation and growth of discrete 3D nuclei. Afterwards, when the individual diffusion zones of adjacent nuclei overlap, the current density reaches a maximum followed by a decaying portion converging to a limiting current, which corresponds to linear diffusion of the electroactive ions to a planar electrode. Therefore, this behaviour follows the usual $t^{-1/2}$ dependence according to the Cottrell equation. This last part of the transients could be modelled using the Heerman and Tarallo approach [11] in order to determine the number of active sites over the substrate surface, N_0, and the nucleation rate constant, A, according to the Eq. (1):

$$i_{3D}(t) = zFDc\frac{1}{(\pi Dt)^{1/2}}\frac{\Phi}{\Theta}\left\{1 - \exp\left[-\alpha N_0(\pi Dt)^{1/2}t^{1/2}\Theta\right]\right\} \quad (1)$$

where

$$\Phi = 1 - \frac{\exp(-At)}{(At)^{1/2}}\int_0^{(At)^{1/2}} \exp(\lambda^2)\mathrm{d}\lambda \quad (2)$$

$$\Theta = 1 - \frac{(1 - e^{-At})}{At} \quad (3)$$

with $\alpha = 2\pi(2MDc/\rho)^{1/2}$, zF: molar charge transferred during electrodeposition, c: metal ion bulk concentration, M: molar mass of the deposit, D: diffusion coefficient, ρ: deposit density and t: time. The function Φ is directly related to the Dawson's integral and reflects the retardation of the current by slow nucleation, and Θ reflects the retardation of the growth of the surface coverage as a result of slow nucleation.

In relation to the deposition peak recorded at short times, it could be attributed to a two-dimensional (2D) Rh deposition process. This behaviour was not reported before for the deposition of Rh on GC substrates, but similar results were observed by Milchev et al. for the electrodeposition of Rh on Au(1 0 0) [2] indicating the formation of two Rh monolayers before the nucleation and growth of the 3D clusters.

Taking into account these previous considerations, the formation of a 2D Rh phase could be modelled using the

Table 1
Kinetic parameters extracted from the current transients for Rh nucleation on activated GC.

E_k vs. SCE (mV)	K_1 (mA cm^{-2})	K_2 (s^{-1})	$AN_0k_g^2$ (2D) (mol^2 cm^{-6} s^{-3})	$N_0k_g^2$ (2D) (mol^2 cm^{-6} s^{-2})	A (3D) (s^{-1})	$N_0 \times 10^{-6}$ (3D) (cm^{-2})	τ (s)
−300	6.2	18.3	0.398	–	0.966	3.2	0
−340	17.4	76.2	–	0.182	3.021	5.0	0.193
−380	1.2	40.2	–	0.396	2.844	25	0.119
−400	1.9	16.8	–	0.540	2.106	65	0.106

Bewick–Fleischman–Thirsk theory (BFT) [12], which indicates that for a progressive 2D nucleation process the current density follows the equation:

$$i_{2D\text{-}P}(t) = \frac{\pi z F M h A N_0 k_g^2 t^2}{\rho} \exp\left(-\frac{\pi M^2 A N_0 k_g^2 t^3}{3\rho^2}\right) \quad (4)$$

and for an instantaneous 2D nucleation process:

$$i_{2D\text{-}I}(t) = \frac{\pi z F M h N_0 k_g^2 t}{\rho} \exp\left(-\frac{\pi M^2 N_0 k_g^2 t^2}{\rho^2}\right) \quad (5)$$

where k_g is the rate constant of lateral growth for a 2D process, h is the height of a monolayer, and all the other parameters have their usual meaning.

Considering that the 2D and 3D mechanisms are overlapped over an interval of time, a simultaneous solution for both the BFT and Heerman and Tarallo equations was carried out in order to achieve the best fit possible for the experimental transients. Following the procedure described by Philipp and Retter [13] and Palomar-Pardavé et al. [14,15] the total experimental current transients can be described as the sum of individual contributions, i.e.,

$$i_{total}(t) = i_{DL}(t) + i_{2D}(t) + i_{3D}(t) \quad (6)$$

where $i_{DL}(t)$ is the estimation of the current density contribution due to the double-layer effect. Based on a Langmuir-type adsorption–desorption equilibrium [16] $i_{DL}(t)$ can be expressed as:

$$i_{DL}(t) = K_1 \exp(-K_2 t) \quad (7)$$

where K_1 and K_2 are constants determined by fitting the experimental data to the model.

Due to the superposition of both the 2D and 3D processes, a time delay, τ, in the beginning of the 3D process was considered and included in Eq. (1) as another fitting parameter in the form $i_{3D}(t-\tau)$. In the case of the 2D deposition mechanism the fitted parameters were the products $AN_0k_g^2$ and $N_0k_g^2$ for progressive and instantaneous nucleation, respectively, which are the most commonly used parameters for this purpose. The diffusion coefficient, D, corresponding to the reactive species, was calculated by a linearization of the falling part of the transients for long times and high overpotentials, in accordance with the Cottrell equation, resulting a value of $D \approx 6.5 \times 10^{-6}$ cm^2/s, which is in good agreement with previously reported values in similar systems [2,5,6].

Fortunately, the current responses associated with the 2D and 3D depositions could be deconvoluted and, therefore, the corresponding models fitted the transients very well in the potential range analysed. As an example, Fig. 2 displays an experimental transient recorded at E_k = −300 mV and the corresponding theoretical curves obtained using Eqs. (1)–(7). In addition, Table 1 shows the values obtained for all the fitted kinetic parameters at the potentials studied.

As a result of the fitting, the 2D deposition process was found to be progressive in nature for relatively positive E_k values (see Eq. (4)) and turned to be instantaneous at more negative applied potentials (see Eq. (5)).

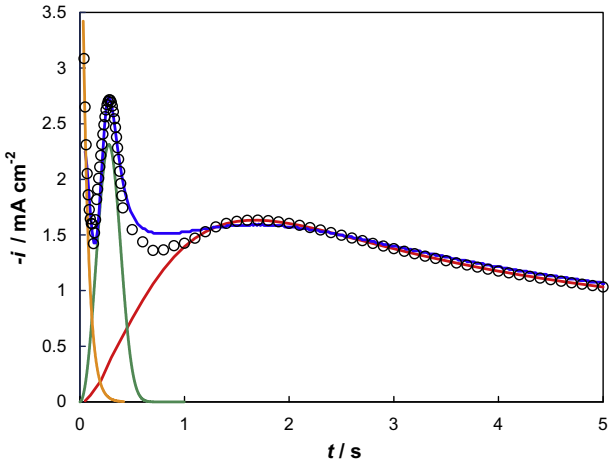

Fig. 2. Experimental current density transient obtained at E_k = −300 mV (——), and the corresponding theoretical curve (○) for the 2D–3D nucleation transition (Eq. (6)). Contributions to the current transient calculated according to Eq. (4) (——), Eq. (1) (——), and Eq. (7) (——) are also shown.

Taking into account the previous results, further studies using a powerful technique such as atomic force microscopy is required in order to characterize the morphology of the Rh deposits at the early stages of deposition, and to correlate it with the electrochemical results. This work is now in progress.

4. Conclusions

In this work, the initial stages of rhodium electrodeposition onto an activated GC substrate from 0.5 M NaCl + 5 mM Na_3RhCl_6 were analysed for the first time. Analysis of the experimental data indicates that the formation of Rh deposits involves a 2D–3D nucleation transition. An initial 2D progressive nucleation is observed at short times, which evolves to a 2D instantaneous nucleation process at more cathodic potentials. In both cases these 2D nucleation processes are followed by a 3D nucleation with diffusion controlled growth at longer times. The theoretical model of Bewick, Fleischman and Thirsk, and the model of Heerman and Tarallo were applied for the first and the second nucleation processes respectively, obtaining in both cases the corresponding kinetic parameters.

Acknowledgements

The authors wish to thank the Universidad Nacional del Sur, Argentina, for the financial support of this work. E.N. Schulz acknowledges a fellowship granted by CONICET.

References

[1] P.M. Tucker, M.J. Waite, B.E. Hayden, J. Appl. Electrochem. 34 (2004) 781.
[2] M. Arbib, B. Zhang, V. Lazarov, D. Stoychev, A. Milchev, C. Buess-Herman, J. Electroanal. Chem. 510 (2001) 67.

[3] R.T.S. Oliveira, M.C. Santos, L.O.S. Bulhoes, E.C. Pereira, J. Electroanal. Chem. 569 (2004) 233.
[4] R. Gómez, F.J. Gutiérrez de Dios, J.M. Feliu, Electrochim. Acta 49 (2004) 1195.
[5] O. Brylev, L. Roué, D. Bélanger, J. Electroanal. Chem. 581 (2005) 22.
[6] D. Pletcher, R.I. Urbina, J. Electroanal. Chem. 421 (1997) 137.
[7] D. Pletcher, R.I. Urbina, J. Electroanal. Chem. 421 (1997) 145.
[8] R.L. McCreery, in: A.J. Bard (Ed.), Electroanalytical Chemistry, vol. 13, Marcel Dekker, New York, 1991.
[9] S. Fletcher, C.S. Halliday, D. Gates, M. Westcott, T. Lwin, G. Nelson, J. Electroanal. Chem. 159 (1983) 267.
[10] B. Scharifker, G. Hills, Electrochim. Acta 28 (1983) 879.
[11] L. Heerman, A. Tarallo, J. Electroanal. Chem. 470 (1999) 70.
[12] A. Bewick, M. Fleischmann, H.R. Thirsk, Trans. Faraday Soc. 58 (1962) 2200.
[13] R. Philipp, U. Retter, Electrochim. Acta 40 (1995) 1581.
[14] M. Palomar-Pardavé, M. Miranda-Hernández, I. González, N. Batina, Surf. Sci. 399 (1998) 80.
[15] M. Palomar-Pardavé, I. González, N. Batina, J. Phys. Chem. B 104 (2000) 3545.
[16] M.H. Holzle, C.W. Apsel, T. Will, D.M. Kolb, J. Electrochem. Soc. 142 (1995) 3741.